2022

Optimization of Intermediate Discharge Valve Positions in a Scroll Compressor with Deep Reinforcement Learning

Janggon Yoo

Taekyeong Jeong

Daegyoum Kim

Optimization of Intermediate Discharge Valve Positions in a Scroll Compressor with Deep Reinforcement Learning

Janggon YOO[1], Taekyeong Jeong[1], Daegyoum KIM[1*]

[1] KAIST, Department of Mechanical Engineering,
Daejeon, Republic of Korea
E-mail : rjg0522@kaist.ac.kr (Janggon Yoo), tkjeong@kaist.ac.kr (Taekyeong Jeong),
daegyoum@kaist.ac.kr (Daegyoum Kim)

* Corresponding Author

ABSTRACT

As seasonal climate changes, modulating the pressure ratio of the scroll compressor is required to operate heating and cooling cycles. Over-compression of a scroll compressor caused by a wide range of operating conditions reduces energy efficiency and gives structural damage to the scroll. Intermediate discharge valves (IDVs) applied in the scroll compressor can avoid over-compression by discharging compressed refrigerant. However, designing the positions of IDVs for proper pressure control without geometric conflict requires time-consuming works due to manual design. This research aims to optimize IDV positions located on a fixed scroll with deep reinforcement learning to maximize the energy efficiency for given scroll design, number of the IDV, and range of operating conditions. An analytical pressure simulation for the scroll compressor, which is based on the energy and mass balance equations, is established as an environment of the reinforcement learning. A proximal policy optimization agent is trained to maximize the summation of adiabatic efficiency for various operating conditions. The geometric conflict of the IDV is considered by using penalty on a reward function, and the reward evolution of the training is presented to show the optimization results. The optimization technique proposed in this study is found to reduce the time cost of developing scroll and IDV design by the automatic design process.

1. INTRODUCTION

Modulation of the scroll compressor's suction-discharge pressure ratio and orbiting frequency is required for a multi-purpose compressor for efficient operation, especially where seasonal climate changes are profound (Winandy & Hundy, 2008; Oquendo et al., 2016). A typical issue arising from the inappropriate operating condition, specifically at a low suction-discharge pressure ratio, is the operating fluid inside the compression chamber being overpressurized above the desired discharge pressure. This excessive compression can cause work loss and structural stress during operation, which decreases the efficiency and reliability of the compressor. In order to remedy the shortcoming, intermediate discharge valves (IDVs) are adopted to let the fluid inside the compression chamber reach appropriate discharge pressure at intermediate stages of compression to be discharged, avoiding overpressurization and the problems it entails (Giniès et al., 2011; Angel et al., 2013; Picavet & Angel, 2016).

The effect of IDVs has been demonstrated mostly with numerical simulations, while some experimental works do exist. The work of Picavet and Ginies (2014) monitors the complete pressurization cycle of the compressor chamber of two compressors, with and without IDVs, using pressure and displacement sensors. While the focus of the work was on the evolution of the pressure inside multiple chamber points, the effect of IDVs in reducing overpressure is demonstrated. Giniès et al. (2011) showed the increase of isentropic efficiency of scroll compressor and reduction of the mechanical load of Oldham coupling. Angel et al. (2013) and Picavet and Angel (2016) presented the flow and pressure field of the scroll compressor with intermediate discharge ports (IDPs) by using an unsteady, turbulent, and compressible CFD model. The fatigue on the Oldham coupling was estimated by Dang Van fatigue analysis, and it shows that IDVs increase the safety factor of the coupling.

In order to further enhance the performance of a scroll compressor, position optimization of IDVs is required. Relevant studies on optimizing the valve positions in the scroll compressors include the work of Cho et al. (2012) presenting the optimal injection port position, and Kim et al. (2017) showing the optimal position considering the seasonal conditions

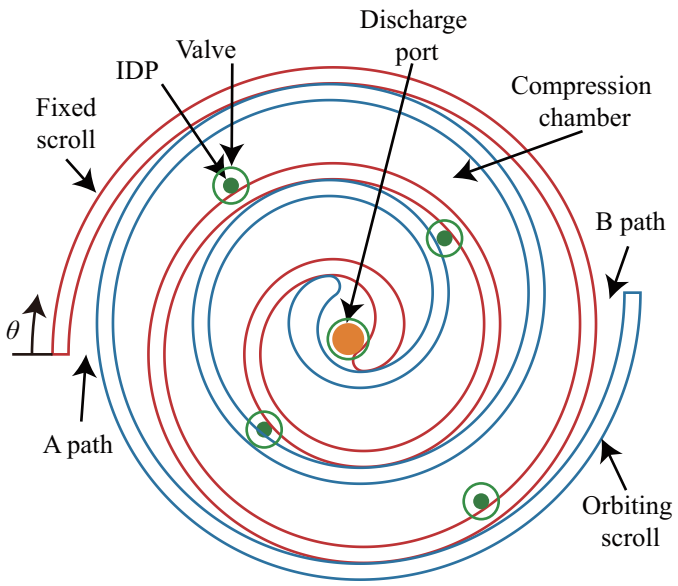

Figure 1: Schematic view of scroll profiles with discharge ports and valves.

with a seasonal coefficient of performance (SCOP). Cavazzini et al. (2020) applied particle swarm optimization (PSO) method to obtain proper discharge port radius with thickness and orbit radius to maximize efficiency.

The efficiency of IDVs is determined by comparing the discharge area and the compression speed of the chamber, which is estimated in orbiting angle domain. Also, Optimizing IDVs requires a geometric restraint inhibiting the valves from being positioned too close to each other, which can be evaluated in a spatial coordinate system. However, such restraint works as a non-linearity of the objective function making gradient-based optimization improper for this problem. Moreover, the gradient-based optimization requires enormous computation resources, and it shows convergence easily on local maximum points. To overcome the limitations, we present deep reinforcement learning (DRL) based optimization, which can deal with non-linear phenomena properly.

The objective of RL is to find proper actions from given states for maximum rewards by using an interaction loop with the agent and environment. DRL is one of the algorithms of RL, which adopts deep learning for the agent to choose actions and predict rewards. DRL properly studies the non-linear and multiple degree-of-freedom (DOF) systems by using deep learning. Thus, DRL becomes one of the proper solutions for complicated shape optimization. Yan et al. (2019) proposed DRL-based shape optimization of fins of a missile to maximize lift-drag ratio. The deep deterministic policy gradient (DDPG) method is adopted as an optimizer, and aerodynamic prediction software and computational fluid dynamics work as the environment. Qin et al. (2021) presented multi-objective shape optimization of blade airfoils in turbo-machinery to minimize pressure loss and maximize laminar flow area. Qin et al. (2021) also applies DDPG and CFD for optimization, and weights are adopted to make objectives as a single reward. Viquerat et al. (2021) showed optimization of a single airfoil's lift-drag ratio with proximal policy optimization (PPO) and CFD. Degenerate DRL, which has a single time-step per episode, is applied to optimize the airfoil shape reconstructed by Bézier curves,

This paper presents a method to locate IDVs in optimal positions to minimize the compression work using DRL. The methodology chapter will treat the geometry generation of the scroll, the analytic model for the compression process, and the optimization method. Optimization results will be suggested in the results section, followed by the conclusions section summarizing the study's key findings.

2. METHODOLOGY

2.1 Geometry of the scroll compressor

The complete mesh profile (CMP) method is applied to generate an involute-based scroll compressor (Wang et al., 2018). The midline of the scroll compressor profile consists of arcs at the inner part and involutes at the outer part of the profile. The fixed and orbiting scroll are spaced by half the orbiting radius from the midline. Figure 1 shows the

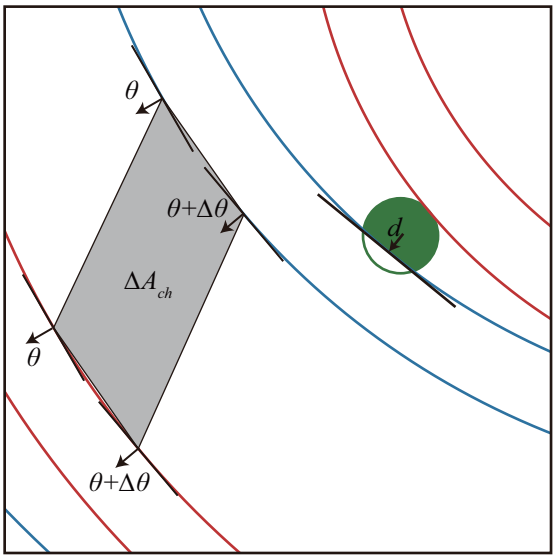

Figure 2: Infinitesimal area of the compression chamber and opening of IDV.

profile of the scroll compressor, and the parameters for the geometry of the scroll are listed in Table 1. The angular coordinate (θ) represents a contact point for a given orbiting angle and a parameter to locate IDVs.

As the orbiting scroll is linearly translated, multiple contact points are produced, and the contact points move toward the central point through the surface of the fixed scroll. Compression chambers surrounded by the fixed and orbiting scroll are generated between two contact points, and they move and shrink while the scroll compressor operates. The compression chambers starting from the tip of the fixed and orbiting scrolls are defined as A and B paths, respectively. Furthermore, the compression chamber at the discharge port is called a discharge chamber.

The volume of the compression chamber is evaluated using the area between infinitesimal arcs (Figure 2). The area between two arcs within the infinitesimal normal angle ($\Delta\theta$) can be expressed by the area between concentric arcs and the size of a trapezoid induced by a displacement of the center of the orbiting scroll. It can be simplified by using the orbiting radius (r_{orbit}) and the radius of curvature of the midline (r_{mid}). The total area of the compression chamber can be numerically evaluated, and the volume can be estimated by multiplying the total area and height of the compressor (h).

$$V_{ch} = h \sum \frac{1}{2} r_{orbit} r_{mid} [1 - \cos(\varphi - \theta)] \Delta\theta \tag{1}$$

Positions of the IDVs are determined by θ and deviation from the fixed scroll profile (d).

Table 1: Specifications of the scroll compressor

Parameter	
Base circle radius (mm)	5
Thickness (mm)	5.24
Height (mm)	40
Involute end angle (Deg)	1260
Modified involute angle (Deg)	90
Radius of IDV port (mm)	2.6
Radius of discharge port (mm)	5
Radius of IDV (mm)	5.2

$$x = x_{fix} - d\cos\theta \tag{2}$$

$$y = y_{fix} - d\sin\theta \tag{3}$$

When calculating the opening area of an IDV, the scroll is assumed to be a straight line because the radius of curvature of the scroll is more significant than ten times of radius of corresponding intermediate discharge ports (IDPs). The open area of an IDV can be evaluated by the distance between the straight line and the center of IDVs (Equation 4).

$$A_{IDV} = \begin{cases} 0 & \text{for} \quad d < -r_{IDP} \\ r_{IDP}^2 \cos^{-1}\left(\frac{d}{r_{IDP}}\right) + d\sqrt{r_{IDP}^2 - d^2} & \text{for} \quad -r_{IDP} < d < r_{IDP} \\ \pi r_{IDP}^2 & \text{for} \quad d > r_{IDP} \end{cases} \tag{4}$$

The opening area of the central discharge port is evaluated by changing the central discharge port and the compression chamber as polygons and applying the polygon intersection area calculation algorithm in the Python Shaply package. The chamber volume and the discharge area are sampled for every single degree of normal angle.

2.2 Analytic model for compression process

We can predict the pressure inside the compression chamber during the compressor operation by using mass and energy balance equations with open control volume (Chen et al., 2002). The change of specific volume inside the compression chamber is determined by the volume change and discharging mass flux through the valves. Isentropic and one-dimensional compressible nozzle flow is assumed to derive discharge mass flow. The discharged mass flow rate can be determined by the pressure and temperature of the chamber, opening area through the discharge port, and Mach number across the discharge port. The Mach number can be derived from the pressure ratio through the discharge port, but is restricted not to become larger than 1, called a choked flow.

The energy balance equation determines the temperature and pressure changes during the compression process with the change of specific volume. To simplify the analytic model for the compression process, we neglect leakage and heat transfer between scroll and compression chamber, which means that the influx enthalpy is neglected. Then, the derivations of temperature and pressure are proportional to the change of specific volume.

The temperature and pressure have equilibrium states when the volume compression and mass flux meet a balance, so the change of the specific volume becomes zero. The pressure becomes slightly larger than the discharge pressure to make the mass flux equilibrium state. If the discharge area is small, the equilibrium pressure increases significantly to maintain the mass flux. It is one of the reasons for the over-pressurization.

The mass, pressure, and temperature during the compression process can be determined using the fourth-order Runge-Kutta method. The drastic pressure reduction during the discharge process leads to numerical error if the time step is too significant. For example, if the pressure and the time step are large enough, the pressure at the next time step can become lower than the discharge process. In that case, the chamber repeats the compression and discharge process, and the pressure-orbiting angle graph shows a serrated shape called a stiff system. We applied the dynamic time-step method to prevent the calculation error, whose time step is proportional to the time it takes to reach the discharge pressure.

The compression chambers from the A and B paths merge at the discharge port, and the fluid in both chambers is mixed together. The fluid is assumed to be homogeneous in the mixed chamber, and total mass and enthalpy are conserved.

2.3 Optimization with DRL

The RL method can be divided into value-based RL and policy-based RL. The value-based RL predicts the expected reward from given states and actions and selects the action that makes the reward maximum. The value-based RL is improper for continuous action space because the algorithm requires too many resources to predict all rewards from the continuous action. In contrast, policy-based RL finds optimal policy directly. The action is determined probabilistically by policy, so the computational resource to choose the action is less required than a value-based function. The PPO algorithm, one of the actor-critic methods, is applied in this study by merging the two methods.

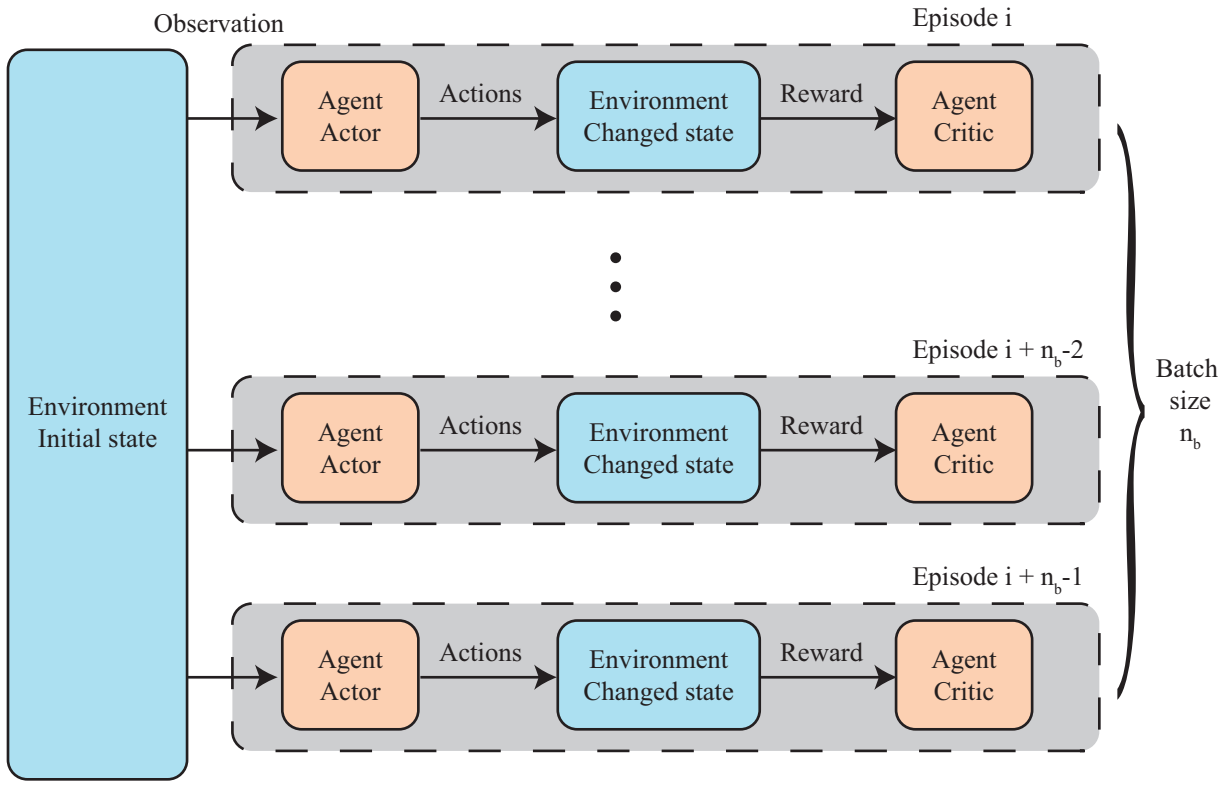

Figure 3: Reinforcement learning framework

In the actor-critic method, the policy-based method (actor) chooses the action, and the value-based method (critic) evaluates the actions.

In this study, degenerated version of the PPO algorithm, proposed by (Viquerat et al., 2021), is applied to optimize the position of IDVs in the scroll compressor. A framework of the algorithm is proposed in Figure 3. Observing the initial environment state, the actor in the agent returns actions. With the action, the positions of IDVs are changed, and the environment calculates the pressure and reward. Then, the critic of the agent evaluates the actions, and the agent's policy is modified. Learning rate and batch size are 10^{-3} and 320, respectively.

This method has a single running step for an episode so that the action can change the environment only at the initial stage of the episode. Therefore, this method is appropriate for position optimization of IDVs because the positions of the IDVs are fixed on the compressor body.

IDVs are classified into two categories depending on whether the position can be changed during the optimization process. The IDVs whose positions can be changed are named as free IDVs, and the IDVs whose positions are fixed are named as fixed IDVs. The individual positions of the free IDVs are determined by the actions assigned with each IDV, whose range is $[0, \theta_{max}]$. The degree of freedom is the same as the number of free IDVs. The deviation from the fixed scroll (d) is restricted to have a minimum value because it is obvious to have a maximum discharge area through the compression process.

Table 2: Specifications of the scroll compressor

operating condition	P_d/P_s	orbiting frequency	$\theta(P = P_d)$	weight
Condition 1	2.0	60	316	0.25
Condition 2	2.5	90	389	0.5
Condition 3	3.0	120	440	0.25

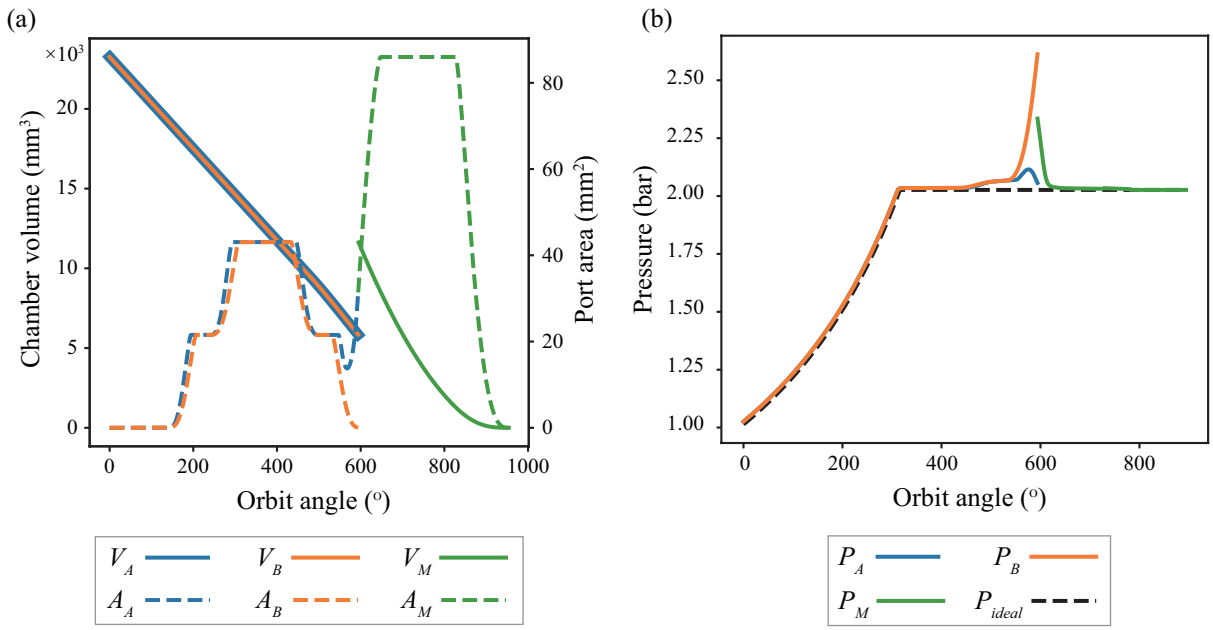

Figure 4: (a) Chamber volume and port area of the scroll compressor and (b) pressure of the compression chamber with respect to orbit angle. Suction-discharge pressure ratio is 2. The IDVs are located at θ = 500° and 600° for both A and B paths.

After new positions of the IDVs are determined, the environment runs the analytic model to derive the pressure inside the chamber for the compression process as described in section 2.2. Required work to compress the coolant, the objective function to minimize, can be estimated using the pressure. In order to consider the modulation of the working condition for SCOP, three operating conditions are considered (Table 2), and the weights for each condition are applied to the works.

Because the RL method is trained to maximize the reward, reduced work consumption by adding the IDVs is taken as an objective function (5). However, if the distance between two IDVs is closer than the diameter of the IDV head, the reward becomes zero because the valves are geometrically conflicted.

$$r_t = \begin{cases} W_{no\ IDV} - \sum w_i W_i & \text{if the valves are not geometrically conflicted} \\ 0 & \text{if the valves are geometrically conflicted} \end{cases} \tag{5}$$

where, w means weight factor and i denotes the operating condition index.

3. RESULTS

3.1 Analytic model result

An example of the area calculation and pressure estimation through the chapter 2.1 and 2.2 with four IDVs located at 500 and 600 degrees (Figure 1) is presented at Figure 4. The operating condition is condition 1 (Table 2), and the pressure is compared with the ideal pressure. Near θ = 600°, the port area decreases because the central discharge port is opened only at the A path. As a result, the equilibrium between mass flux and volume change is broken, and over-pressurization occurs. After the mixing procedure, the discharge port leaks out the over-compressed fluid inside the discharge chamber. Therefore, the pressure becomes an equilibrium state again. A sufficient port area is necessary for these phenomena after the pressure becomes larger than the discharge pressure. In our wrap design, the pressure become discharge pressure at 300, 350, and 400 for the pressure ratio is 2.0, 2.5, and 3.0, respectively. It means that the IDVs should be located near the center of the scroll.

3.2 Position optimization results

A reward evolution and an optimization result obtained by the DRL configuration with six free IDVs are presented in Figure 5. In the reward evolution (Figure 5a), the non-linearity of objective function caused by the geometric restriction

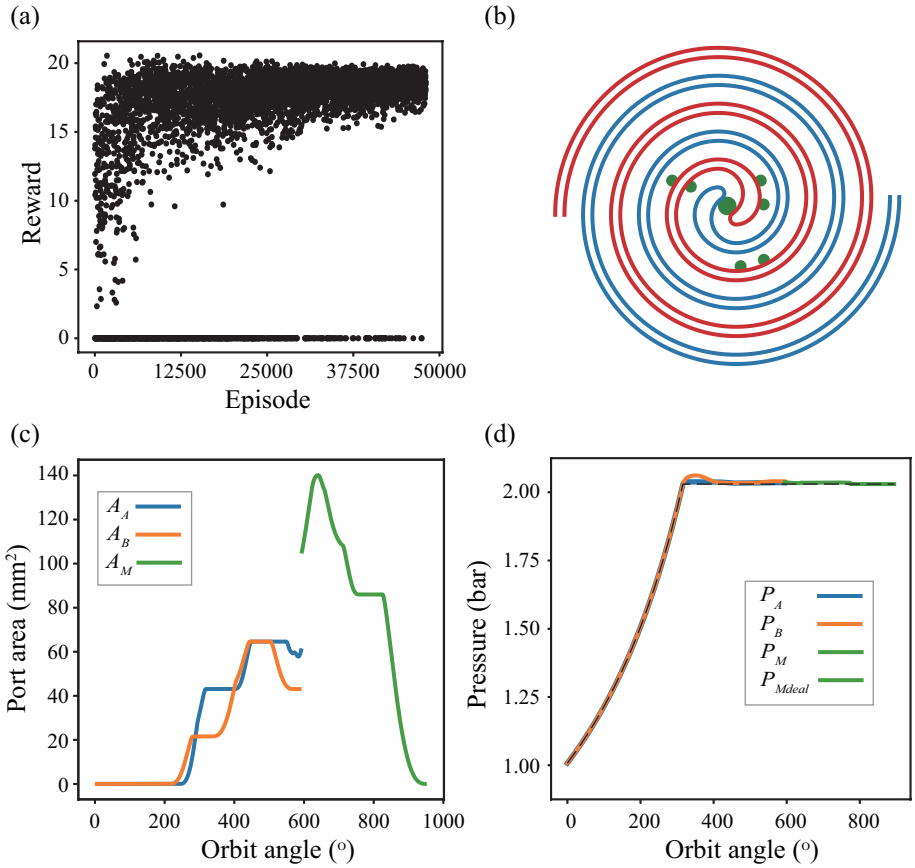

Figure 5: Example of the optimal positions of IDVs and corresponding discharge area and pressure: (a) reward evolution with six IDVs, (b) scroll profiles with optimal discharge ports, (c) port area of the scroll compressor, and (d) pressure of the compression chamber with respect to orbit angle for operating condition 1 (P_d/P_s = 2.0 and f = 60 Hz).

(Equation 5) is appeared as zero reward. During training, the reward grows drastically until 10000 episodes and slowly converges to 20. Moreover, It can be seen that the frequency of exceptions gradually decreases and eventually disappears at episode 50000, which means the agent learns the non-linear system properly.

As a result of the optimization, the positions of IDVs and the corresponding discharge area are shown in Figures 5b and 5c. All IDVs are assigned near the discharge area to make enough discharge area after the angle where the chamber starts to discharge (see Table 2). However, near 300°, the port area at the B path is not enough, so the fluctuation of pressure can be observed (Figure 5d). After that region, the pressure meets the ideal pressure line for all paths. Moreover, The B path of the scroll chamber has two IDVs right before the center discharge port, but the A path has only one IDV in the same region. It is reasonable because the center discharge port is opened only at the A path before the mixing occurs (Figure 4a), so the B path requires more discharge area near the discharge chamber than the A path.

Figure 6 shows the position optimization of IDVs with different DOF by fixing some IDVs. The free IDVs are positioned near the center of the scroll compressor to maximize the discharge area after 316 degrees (Figure 6a, b, and c). The fixed IDVs are located at the same angle for both A and B paths, and the positions are 180° for both two- and four-DOF cases and 540° only for two- DOF cases. In a two-DOF optimization case, the pressure fluctuation appears before the mixing occurs (Figure 6d). It means that the discharge area of a single IDV is not sufficient to maintain the pressure lower. In four-DOF optimization cases, the pressure is almost the same as discharge pressure in operating conditions 2 and 3. However, the over-pressurization is observed at 320° but quickly goes to discharge pressure after 400° for working condition 1 (Figures 6e). This phenomenon is caused by the weight factor and the initial discharge angle of each operating case (Table 2. The weight increases from 0.25 to 0.75, with 389 degrees as the boundary. As

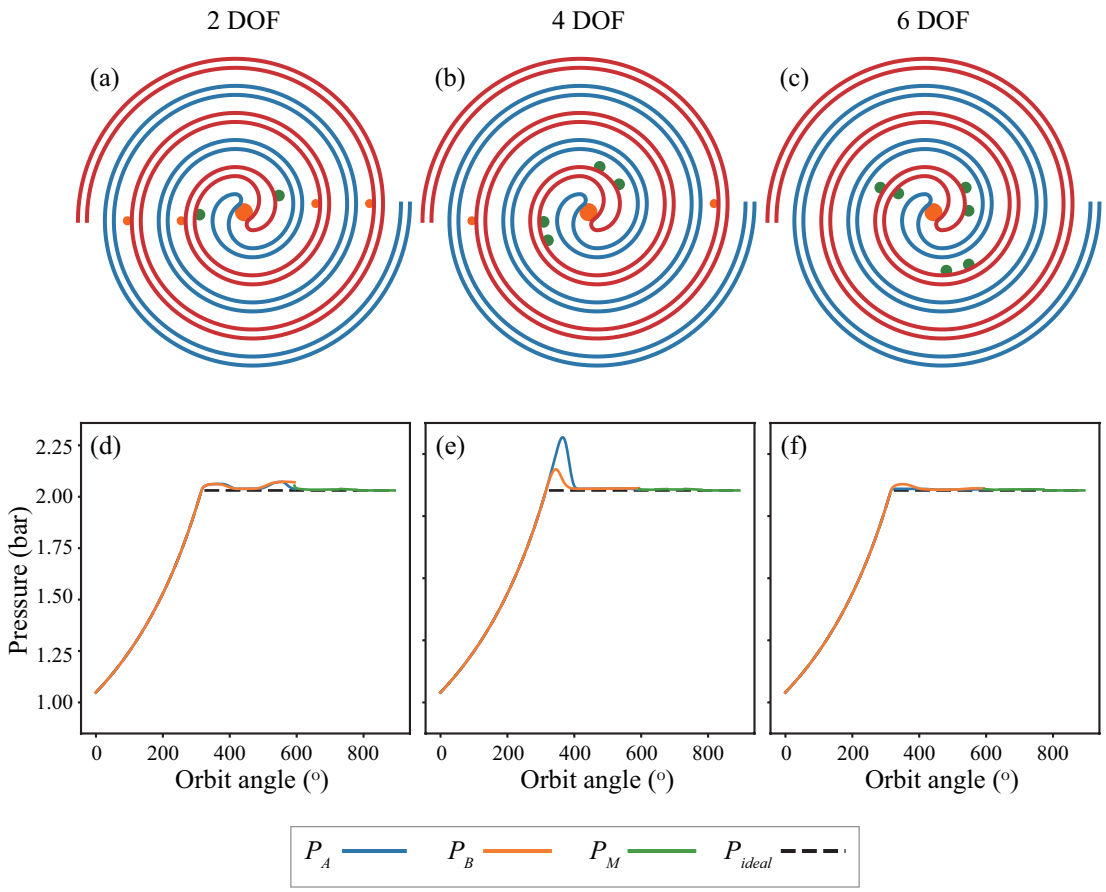

Figure 6: Optimal locations of IDVs (first row) and corresponding pressure along orbit angle under operating condition 1 (second row) for different DOF systems: (a and d) two DOFs; (b and e) four DOFs; (c and f) six DOFs. Operating condition is P_d/P_s = 2.0 and f = 60 Hz. Orange circles in the schematics denote fixed IDVs, and green circles denote free IDVs.

a result, the agent becomes less concerned about the angle before 389 degrees in the four-DOF optimization case. In contrast, in the six-DOF optimization case, the discharge area after 316 degrees is fully covered by the IDVs. The equilibrium pressure is small enough with two IDVs, and it will decrease slightly with additional IDV. As a result, the pressure is stabilized throughout the condition by assigning the additional IDVs at a lower angle (Figures 6f).

4. CONCLUSIONS

In this work, we present the optimization method of the positions of the IDVs in an involute-based scroll compressor with an analytic pressure model. The scroll compressor design method, chamber area, and discharge port estimation method are proposed. The area determines the pressure and compression work, and the work becomes the objective function to minimize. The PPO-based optimization method is applied to the objective function with various operating conditions. As a result, the optimal position of IDVs to minimize compression works and avoid geometric restriction for various operating conditions and the number of the free IDVs are presented. From the reward evolution, the PPO agent is validated for the training performance of the system with a non-linear objective function well.

This contribution is significant in terms of the combination of the analytic compressor model and the DRL method for shape optimization. This method is suitable for industrial purposes since it can deal with the non-linear aspect and produce optimization results fast by using parallel training. Also, this method can be extendable to various shape optimization such as injection port position optimization and discharge port shape optimization.

NOMENCLATURE

A	area	(m^2)
h	height of scroll	(m)
d	distance	(m)
r	radius of curvature of scroll	(m)
x	cartesian coordinates	(m)
y	cartesian coordinates	(m)
P	pressure of compression chamber	(Pa)
V	volume of compression chamber	(m^3)

Greek letter

θ	normal angle of scroll	(rad)

Subscript

A	A path
B	B path
ch	chamber
IDP	center discharge port
IDV	intermediate discharge valve
mid	midline
orbit	orbit

REFERENCES

Angel, B., Ginies, P., Gross, D., & Ancel, C. (2013). Cfd modelling of scroll compressor intermediate discharge ports. In *8th international conference on compressors and their systems* (p. 613-623). Woodhead Publishing.

Cavazzini, G., Giacomel, F., Ardizzon, G., Casari, N., Fadiga, E., Pinelli, M., … Montomoli, F. (2020). CFD-based optimization of scroll compressor design and uncertainty quantification of the performance under geometrical variations. *Energy*, *209*, 118382.

Chen, Y., Halm, N. P., Groll, E. A., & Braun, J. E. (2002). Mathematical modeling of scroll compressors - Part I: Compression process modeling. *Int. J. Refrig.*.

Cho, I. Y., Bin Ko, S., & Kim, Y. (2012). Optimization of injection holes in symmetric and asymmetric scroll compressors with vapor injection. *Int. J. Refrig.*, *35*(4), 850–860.

Giniès, P., Ancel, C., & Gross, D. (2011). Scroll compressors and intermediate valve ports. In *7th international conference on compressors and their systems 2011* (p. 477-488). Woodhead Publishing.

Kim, D., Chung, H. J., Jeon, Y., Jang, D. S., & Kim, Y. (2017, sep). Optimization of the injection-port geometries of a vapor injection scroll compressor based on SCOP under various climatic conditions. *Energy*, *135*, 442–454.

Oquendo, F. M. T., Peris, E. N., Macia, J. G., & Corberán, J. (2016). Performance of a scroll compressor with vapor-injection and two-stage reciprocating compressor operating under extreme conditions. *Int. J. Refrig.*, *63*, 144–156.

Picavet, A., & Angel, B. (2016). Numerical simulation of the flow inside a scroll compressor equipped with intermediate discharge valves. *International Compressor Engineering Conference*, 2421.

Picavet, A., & Ginies, P. (2014). Experimental pressure-volume diagrams of scroll compressors. *International Compressor Engineering Conference*.

Qin, S., Wang, S., Wang, L., Wang, C., Sun, G., & Zhong, Y. (2021). Multi-objective optimization of cascade blade profile based on reinforcement learning. *Appl. Sci.*, *11*(1), 1–27.

Viquerat, J., Rabault, J., Kuhnle, A., Ghraieb, H., Larcher, A., & Hachem, E. (2021). Direct shape optimization through deep reinforcement learning. *J. Comput. Phys.*, *428*, 110080.

Wang, J., Liu, Q., Cao, C., Wang, Z., Li, Q., & Qu, Y. (2018). Design methodology and geometric modeling of complete meshing profiles for scroll compressors. *Int. J. Refrig.*, *91*, 199–210.

Winandy, E., & Hundy, G. (2008). Refrigerant and scroll compressor options for best performance of various european heat pump configurations. *International Compressor Engineering Conference*.

Yan, X., Zhu, J., Kuang, M., & Wang, X. (2019). Aerodynamic shape optimization using a novel optimizer based on machine learning techniques. *Aerosp. Sci. Technol.*, *86*, 826–835.

ACKNOWLEDGMENT

This research was supported by the Human Resources Program in Energy Technology of the Korea Institute of Energy Technology Evaluation and Planning (KETEP) granted financial resource from the Ministry of Trade, Industry & Energy, Republic of Korea (No. 20204030200050).